

STUDY OF THE PROCESS $e^+e^- \rightarrow 3(\pi^+\pi^-)$ IN THE C.M.ENERGY RANGE 1.5–2.0 GEV WITH THE CMD-3 DETECTOR

R.R.Akhmetshin^a, A.V.Anisenkov^a, S.A.Anokhin^{a,b},
 V.M.Aulchenko^{a,b}, V.S.Banzarov^a, L.M.Barkov^a, N.S.Bashtovoy^a,
 D.E.Berkaev^{a,b}, A.E.Bondar^{a,b}, A.V.Bragin^a, S.I.Eidelman^{a,b},
 D.A.Epifanov^{a,f}, L.B.Epshteyn^{a,c}, G.V.Fedotov^{a,b},
 S.E.Gayazov^{a,b}, A.A.Grebenuk^{a,b}, D.N.Grigoriev^{a,c},
 E.N.Gromov^a, F.V.Ignatov^a, S.V.Karpov^a, V.F.Kazanin^{a,b},
 B.I.Khazin^{a,b}, I.A.Koop^{a,b}, A.N.Kozyrev^a, P.P.Krokovny^{a,b},
 A.E.Kuzmenko^{a,c}, A.S.Kuzmin^a, I.B.Logashenko^{a,b}, A.P.Lysenko^a,
 P.A.Lukin^{a,b}, K.Yu.Mikhailov^a, Yu.N.Pestov^a,
 E.A.Perevedentsev^{a,b}, S.A.Pirogov^a, S.G.Pivovarov^a,
 A.S.Popov^{a,b}, Yu.S.Popov^a, S.I.Redin^a, Yu.A.Rogovsky^a,
 A.L.Romanov^a, A.A.Ruban^a, N.M.Ryskulov^a,
 A.E.Ryzhenenkov^{a,b}, V.E.Shebalin^a, D.N.Shemyakin^{a,b},
 B.A.Shwartz^{a,b}, D.B.Shwartz^a, A.L.Sibidanov^{a,d}, P.Yu.Shatunov^a,
 Yu.M.Shatunov^a, I.G.Snopkov^a, E.P.Solodov^{a,b,1}, V.M.Titov^a,
 A.A.Talyshev^{a,b}, A.I.Vorobiov^a, Yu.V.Yudin^a, A.S.Zaytsev^{a,e}

^a*Budker Institute of Nuclear Physics, SB RAS, Novosibirsk, 630090, Russia*

^b*Novosibirsk State University, Novosibirsk, 630090, Russia*

^c*Novosibirsk State Technical University, Novosibirsk, 630092, Russia*

^d*University of Sydney, School of Physics, Falkiner High Energy Physics,
 NSW 2006, Sydney, Australia*

^e*Brookhaven National Laboratory, P.O. Box 5000 Upton, NY 11973-5000,
 USA*

^f*University of Tokyo, Department of Physics, 7-3-1 Hongo Bunkyo-ku
 Tokyo, 113-0033, Japan*

Abstract

¹Corresponding author:solodov@inp.nsk.su

The cross section of the process $e^+e^- \rightarrow 3(\pi^+\pi^-)$ has been measured using 22 pb^{-1} of integrated luminosity collected with the CMD-3 detector at the VEPP-2000 e^+e^- collider in the c.m. energy range 1.5 – 2.0 GeV. The measured cross section exhibits a sharp drop near the $p\bar{p}$ threshold. A first study of dynamics of six-pion production has been performed.

1. Introduction

Production of six pions in e^+e^- annihilation was studied at DM2 [1] and with much larger effective integrated luminosity at BaBar [2], using Initial-State Radiation (ISR) events. The DM2 experiment observed a “dip” in the cross section at about 1.9 GeV, confirmed later by the FOCUS Collaboration in the photoproduction [3, 4] and by the BaBar Collaboration, where this structure was also observed in the $2(\pi^+\pi^-)\pi^0\pi^0$ final state [2]. The origin of the “dip” remains unclear, but the most popular explanation suggests a presence of the under-threshold proton-antiproton ($p\bar{p}$) resonance. This hypothesis is supported by the fast increase of the $p\bar{p}$ form factor to the threshold, recently confirmed by the high-statistics BaBar study [5], and discussed in many theoretical papers (see, e.g., Ref. [6]). Even earlier, a narrow structure near the proton-antiproton threshold has been also observed in the total cross section of e^+e^- annihilation into hadrons in the FENICE experiment [7].

The $e^+e^- \rightarrow 3(\pi^+\pi^-)$ cross section is also used in the calculation of the hadronic contribution to the muon anomalous magnetic moment [8]. The detailed study of the production dynamics can further improve the accuracy of these calculations and help in explaining the cross section anomaly.

In this paper we report the analysis of the data sample based on 33 pb^{-1} of integrated luminosity collected at the CMD-3 detector in the 1.0-2.0 GeV center-of-mass energy range. We observe only a few candidate events below 1.5 GeV. Since their number is consistent with background, we present our results for the 1.5-2.0 GeV center-of-mass energy range, corresponding to 22 pb^{-1} of integrated luminosity. These data were collected in three energy scans performed at the VEPP-2000 collider [9].

The general purpose detector CMD-3 has been described in detail elsewhere [10]. Its tracking system consists of a cylindrical drift chamber (DC) [11] and double-layer multiwire proportional Z-chamber, both also used for a trigger, and both inside a thin ($0.2 X_0$) superconducting solenoid with a field of 1.3 T. The liquid xenon (LXe) barrel calorimeter with $5.4 X_0$ thickness has fine electrode structure, providing good spatial resolution [12], and shares the cryostat vacuum volume with the superconducting solenoid. The barrel CsI crystal calorimeter with thickness of $8.1 X_0$ is placed outside the LXe calorimeter, and the end-cap BGO calorimeter with a thickness of $13.4 X_0$ is placed inside the solenoid [13]. The luminosity is measured using events of Bhabha scattering at large angles [14].

2. Selection of $e^+e^- \rightarrow 3(\pi^+\pi^-)$ events

Candidates for the process under study are required to have five and more charged-particle tracks with the following “good” track definition:

- A track contains more than five hits in the DC.
- A track momentum is larger than 40 MeV/c.
- A minimum distance from a track to the beam axis in the transverse plane is less than 0.5 cm.
- A minimum distance from a track to the center of the interaction region along the beam axis Z is less than 10 cm.
- A track has a polar angle large enough to cross half of the DC radius.

The number of events with seven or more selected tracks is found to be less than 1%. Reconstructed momenta and angles of the tracks for six-track and five-track events were used for further selection.

For six- or five-track candidates we calculate the total energy and total momentum assuming all tracks to be pions:

$$E_{\text{tot}} = \sum_{i=1}^{5,6} \sqrt{p_i^2 + m_\pi^2}, \quad P_{\text{tot}} = \left| \sum_{i=1}^{5,6} \vec{p}_i \right|.$$

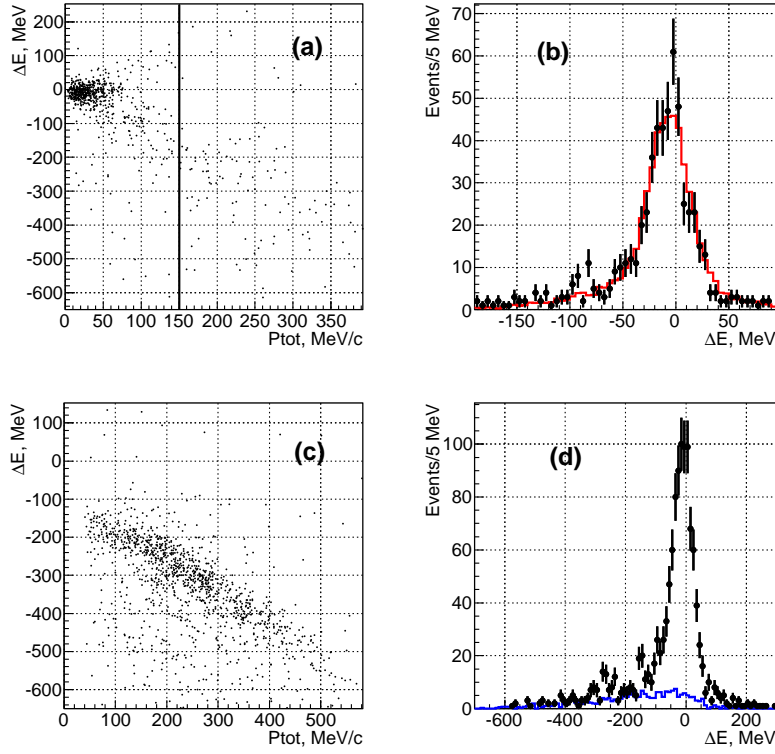


Figure 1: (a) Scatter plot of the difference (ΔE) between the total energy and c.m. energy versus total momentum for six-track events. The line shows the boundary of the applied selection; (b) Projection plot of (a) after selection. The histogram shows the normalised MC-simulated distribution; (c) Scatter plot of difference (ΔE) of total energy and c.m. energy versus total momentum for five-track events; (d) Difference between the total energy of five-tracks plus missing track energy and c.m. energy (points). The histogram shows the distribution for the MC simulated background events (see text).

Figure 1(a) shows a scatter plot of the difference between the total energy and c.m. energy $\Delta E = E_{\text{tot}} - E_{\text{c.m.}}$ versus total momentum for six-track candidates. The histograms combine events from three highest energy points. A clear signal of six-pion events is seen as a cluster of dots near zero. Events with a radiative photon have non-zero total momentum and total energy which is always smaller than the nominal one. A momentum of any pion incorrectly reconstructed due to interaction with detector material or DC resolution leads to momentum-energy correlated “tails” in both directions.

We select events with total momentum less than 150 MeV/c and show the difference ΔE in Fig. 1(b). The experimental points are in good agreement with the corresponding Monte Carlo (MC) simulated distribution shown by the histogram. We require $-200 < \Delta E < 100$ MeV to determine the number of six-pion events. Six-track events have practically no background: we estimate it from MC simulation of the major background processes $2(\pi^+\pi^-\pi^0)$ and $2(\pi^+\pi^-\pi^0)$ (one of the photon from the π^0 decay converts to a e^+e^- pair at the vacuum pipe), and found a contribution of less than 1%. We use this value as an estimate of the corresponding systematic uncertainty.

To determine the number of six-pion events with one missing track, a sample with five selected tracks is used. A track can be lost if it flies at small polar angles outside the efficient DC region, decays in flight, due to incorrect reconstruction, nuclear interactions or by overlapping with another track. Figure 1(c) shows a scatter plot of the difference ΔE between the total energy and c.m. energy versus total momentum for five-track events. Six-pion candidates in the five-track sample have energy deficit correlated with the total momentum. This sample has some admixture of background events from multihadron processes mentioned above with photons from the π^0 decays. We apply an additional requirement on the “neutral” (not associated with charged tracks) energy $E_{neutral}$ in the calorimeter to be less than 300 MeV. This requirement reduces the background by a factor of two and removes less than 2% of signal events estimated using MC simulation.

The direction and momentum of a missing pion can be calculated assuming a six-pion final state. We add energy of a missing pion to the energy of five detected pions and show the difference ΔE in Figure 1(d) by points. A corresponding background distribution from the MC simulation of the $2(\pi^+\pi^-\pi^0)$ and $2(\pi^+\pi^-\pi^0)$ events is shown in Figure 1(d) by the histogram: background events contribute less or about 10% to the signal region after applying a requirement $E_{neutral} < 300$ MeV.

To obtain the number of six-pion events from the five-track sample, we fit the distribution shown in Fig 1(d) with a sum of functions describing a signal peak and background. The signal line shape is taken from the MC simulation

of the six-pion process and is well described by a sum of two Gaussian distributions. The photon emission by initial electrons and positrons is taken into account in the MC simulation and gives a small asymmetry observed in the distributions of Figs. 1 (b,d). We describe this asymmetry by an admixture of a third Gaussian function. All parameter ratios of the signal function are fixed except for the number of events and main Gaussian resolution. The third-order polynomial is used to describe the background distribution.

To estimate a systematic uncertainty of the background subtraction procedure, we compare the MC simulated background distribution with the experimental events with an $E_{neutral} > 300$ MeV requirement, and found reasonable agreement with the histogram shown in Fig 1(d). A variation of the polynomial fit parameters for the experimental and MC simulated background distributions leads to about 3% uncertainty on the number of signal events.

We found 2887 six-track events and 5069 five-track events corresponding to the process $e^+e^- \rightarrow 3(\pi^+\pi^-)$. The numbers of six- ($N_{6\pi}$) and five-track ($N_{5\pi}$) events determined at each energy point are listed in Table 1.

3. First study of the production dynamics

To obtain a detection efficiency, we simulate six-pion production in a primary generator, pass simulated events through the CMD-3 detector using the GEANT4 [15] package, and reconstruct them with the same reconstruction software as experimental data. In our experiment, the acceptance of the DC for the charged tracks is not 100%, and the detection efficiency depends on the production dynamics of six pions. The dynamics of the process $e^+e^- \rightarrow 3(\pi^+\pi^-)$ was not studied previously in detail. The BaBar Collaboration [2] reported the observation of only one $\rho(770)$ from all $\pi^+\pi^-$ invariant mass combinations and no structures in any other (three-, four-pion) invariant mass combinations.

We investigate a few production mechanisms, and compare simulated angular and invariant mass distributions with those in data. All studied distributions strongly contradict to a phase space model, which assumes all

pions to be completely independent. We exclude the phase space model from further consideration. In this paper we illustrate our study with three models, all with one $\rho(770)$ per event. To conserve the initial state quantum numbers, six pions must have $J^{PC} = 1^{--}$.

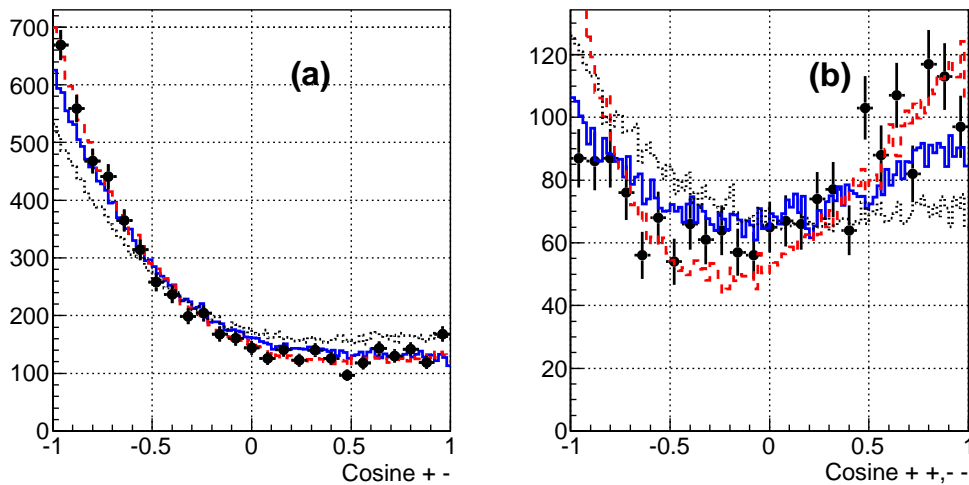


Figure 2: Cosines of the relative angle of two pions with opposite-sign charge (a), and of two pions with same-sign charge (b) for experimental events (dots) and MC simulation for $\rho(1420)\pi^+\pi^- \rightarrow a_1(1260)\pi\pi^+\pi^-$ (dotted histogram), $\rho(770)f_0(1370)$ (solid histogram) and $\rho(770)f_2(1270)$ (dashed histogram).

In the model #1 we use the following decay chain: $e^+e^- \rightarrow \rho(1420)(\pi^+\pi^-)_{S\text{-wave}} \rightarrow a_1(1260)^\pm\pi^\mp\pi^+\pi^- \rightarrow \rho(770)^0 2(\pi^+\pi^-) \rightarrow 3(\pi^+\pi^-)$. This model uses dominant decays $\rho(1420)^0 \rightarrow a_1(1260)^\pm\pi^\mp$ and $a_1(1260)^\pm \rightarrow \rho(770)^0\pi^\pm$ [16], and naturally includes the $a_1(1260)^\pm \rightarrow \rho(770)^\pm\pi^0$ decay to describe the $e^+e^- \rightarrow 2(\pi^+\pi^-\pi^0)$ process with one charged $\rho(770)$ [2]. We use PDG values [17] for the resonance parameters and the model allows to introduce a form factor in each decay vertex.

Another studied model (#2) was simpler: it includes the production of one $\rho(770)^0$ and four pions in S-wave. We try two options: the four pions

are distributed according to the phase space or forming a scalar resonances $f_0(1370)$ or $f_0(1500)$.

And finally, the model (#3) assumes $e^+e^- \rightarrow \rho(770)f_2(1270)$ with a tensor f_2 resonance in the four-pion final state.

MC simulation should reproduce experimental angular distributions of the pions to obtain correct detection efficiency. Figure 2 shows (by points) the cosines of open angles between pions for opposite-sign (a) and same-sign (b) pion pairs for data.

We compare distributions of Fig. 2 with the MC simulated distributions for the model #1 (dotted histogram), model #2 (solid histogram) and model #3 (dashed histogram), and the best agreement was found with the model #2.

Note, that variation of the resonance parameters in the models does not significantly affect these angular distributions. For example, model #2 with production of one $\rho(770)^0$ exhibits the same angular distributions both in the case, when the remaining four pions are distributed according to phase space or form a scalar resonance ($f_0(1370)$ or $f_0(1500)$).

Figure 3(a) presents the polar angle (θ_π) distribution for six-pion events with all detected tracks. The requirement for a track to cross half of the DC radius effectively determines a cut on this parameter. The result of the MC simulation in model #2, presented by the histogram, well describes the observed distribution. Figure 3(b) presents the polar angle distribution for five detected tracks (circles for data, the solid histogram for the MC simulation) after background subtraction. The polar angle distribution for the missing track is shown by squares (data) and the dashed histogram (MC). With our “effective” DC acceptance we have almost two times more six-pion events with one missing track than events with all tracks detected.

We calculate invariant masses for the combinations of two, four (total charge zero), and three (total charge ± 1) pions for the different c.m. energies

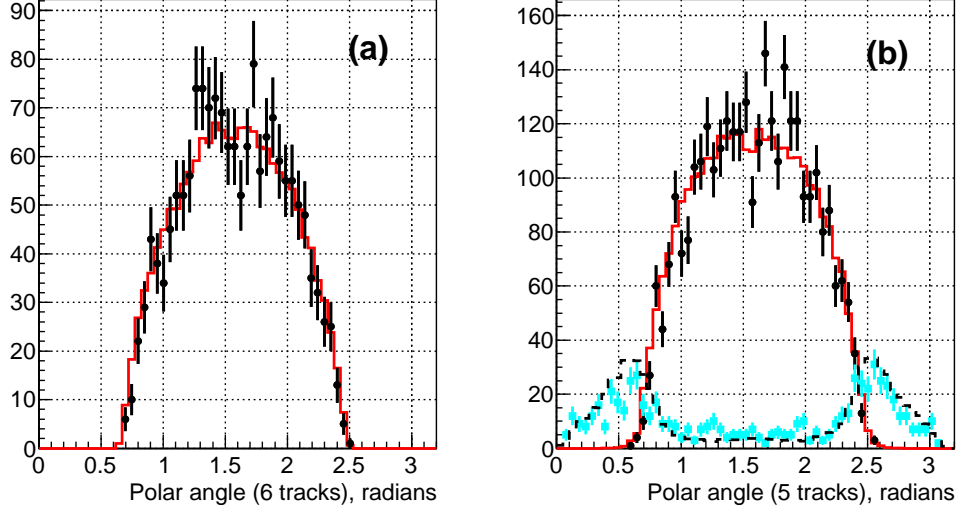


Figure 3: (a) Polar angle distribution for six-pion events with six detected tracks for data (points) and MC simulation (histogram); (b) Polar angle distribution for six-pion events with five detected tracks for data (circles) and MC simulation (solid histogram). The polar angle distribution for a missing track is shown by squares (data) and the dashed histogram (MC simulation).

and show them in Fig. 4. We compare the obtained distributions with model #2 ($\rho 4\pi$), and observe good agreement with experiment at c.m. energies 1600 MeV and 2000 MeV, if four pions are distributed according to phase space (solid histogram). But at the c.m. energy of 1800 MeV the experimental data are better described by the same model with four pions forming $f_0(1370)$. Note that invariant mass distributions for models #1 and #3 do not describe data in any mass interval, but some admixture of these channels cannot be excluded.

From the study of the mass distributions in Fig. 4 we conclude that production dynamics of six charged pions changes in the relatively narrow energy region (1700-1900 MeV). This phenomenon demands a further investigation.

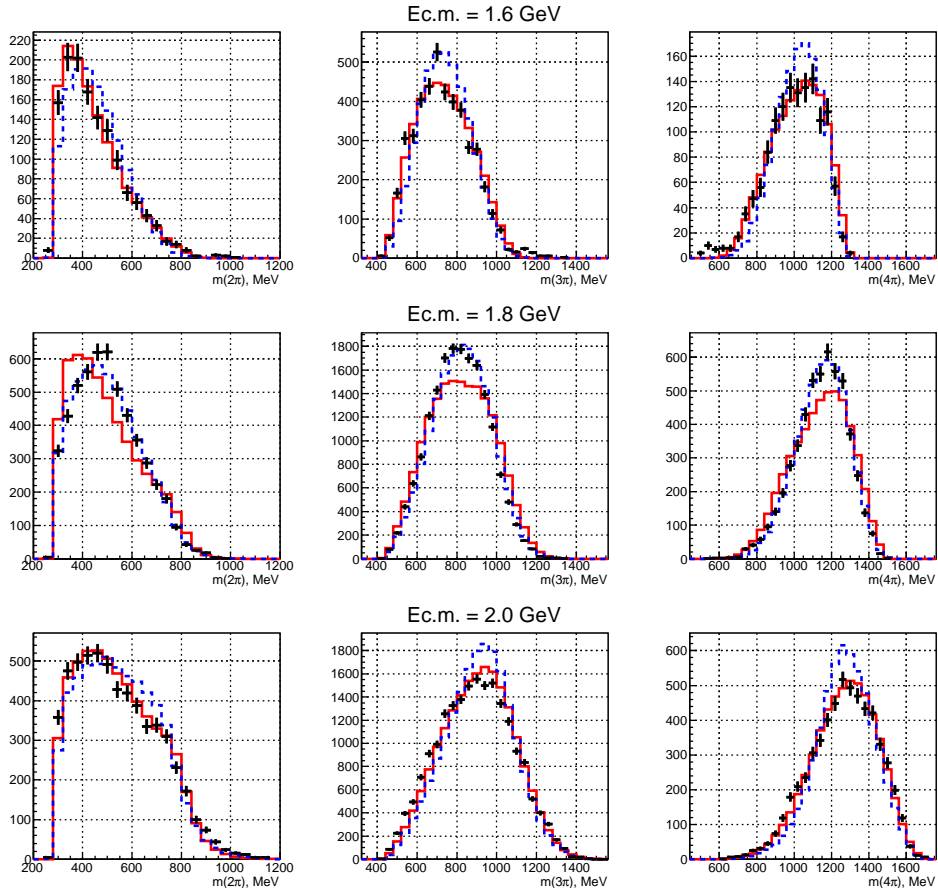


Figure 4: Experimental invariant mass distributions (from left to right) for two, three and four pions for (top to bottom) 1600, 1800 and 2000 MeV c.m. energies in comparison with simulation of one $\rho(770)^0$ with the remaining four pions in S-wave, and distributed according to the phase space (solid histogram) or form a scalar resonance $f_0(1370)$ (dashed histogram).

4. Detection efficiency

We calculate the detection efficiency from the MC simulated events as a ratio of events after selections described in Sec. 2 to the total number of generated events. With the limited DC acceptance, incorrect simulation of the pion angular distribution leads to a systematic error in the efficiency calculation and thus in the cross section measurement.

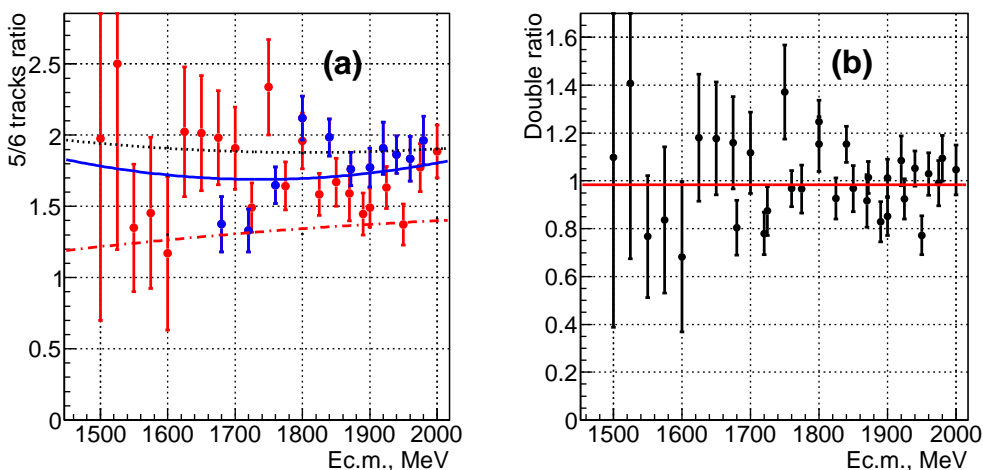


Figure 5: (a) Ratio of events with five and six detected tracks for data (points with errors) and MC simulation for model #1 (dotted line), model #2 (solid line) and model #3 (dashed line); (b) Double ratio $R_{56}^{data}/R_{56}^{MC\#2}$ versus energy. The line shows a fit with a constant.

In the five-track sample, about 15-17% of events have a missing track due to the DC reconstruction inefficiency, well reproduced by the MC simulation. The remaining events migrate from the six- to the five-track sample due to the limited DC acceptance (see Fig. 3). It makes the ratio $R_{56} = N_{5\pi}/N_{6\pi}$ very sensitive to the pion angular distribution, and we study it to validate the model used for the efficiency calculation.

Figure 5 (a) shows the R_{56} ratio versus energy for data (points with errors) and for three models, discussed in Sec. 3. The experimental average value

$R_{56}^{data} = 1.74 \pm 0.03$ is in good agreement with $R_{56}^{MC\#2} = 1.76$ for the model #2 (solid line), but inconsistent with model #1 ($R_{56}^{MC\#1} = 1.92$, dotted line) and model #3 ($R_{56}^{MC\#3} = 1.30$, dashed line). A “naive” phase space model for the six-pion production (all tracks uncorrelated) gives $R_{56}^{MC} = 2.1$.

To estimate a model-dependent systematic error, we compare the experimental number of six- and five-track events after normalisation to the MC simulated acceptance. We calculate a double ratio $R_{56}^{data}/R_{56}^{MC\#2}$ for each energy point for the model #2, and show it in Fig. 5 (b). The average value 0.984 ± 0.018 ($\chi^2/n.d.f=56/35$) is in good agreement with the prediction of model #2 in the studied energy interval, so that a maximum systematic deviation from unity does not exceed 3.4%. However, a relatively large χ^2 value can be an indication of the additional systematic uncertainty, and we conservatively take 4% as an estimate of a systematic error on the detection efficiency using $\sqrt{\chi^2/n.d.f}$ as a scale factor.

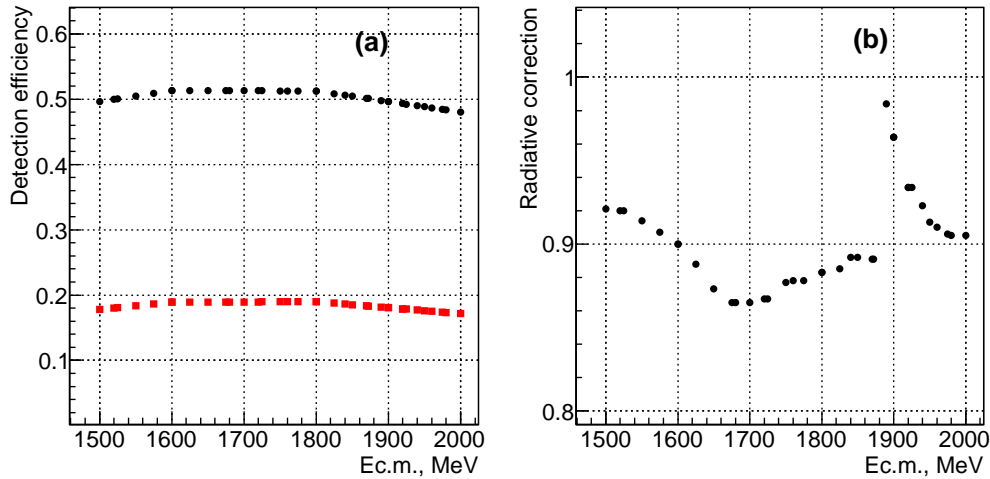


Figure 6: (a) Efficiency calculated from the MC simulation for six-track events (squares) and for a sum of five- and six-track events (circles); (b) Radiative correction.

The detection efficiency thus obtained with model #2 is shown in Fig. 6(a) for events with six detected tracks (squares) and for a sum of five- and six-

track events (circles), increasing efficiency by factor 2.5. Note that if a sum of six- and five-track events ($N_{6\pi} + N_{5\pi}$) is taken for the detection efficiency calculation, the data-MC inconsistencies in the description of the DC inefficiency and (partly) in the model-dependent angular distributions are significantly reduced.

5. Cross Section Calculation

At each energy the cross section is calculated as

$$\sigma = \frac{N_{6\text{tr}} + N_{5\text{tr}}}{L \cdot \epsilon \cdot (1 + \delta)},$$

where L is the integrated luminosity for this energy point, ϵ is the detection efficiency (Fig. 6(a)), and $(1 + \delta)$ is the radiative correction calculated according to [18] and shown in Fig. 6 (b). The energy dependence of the radiative correction reflects a sharp dip in the cross section. To calculate the correction we use BaBar data [2] as a first approximation and then use our cross section data for iterations.

The integrated luminosity, the number of six and five-track events, detection efficiency, radiative correction and obtained cross section for each energy point are listed in Table 1.

6. Systematic errors

The following sources of systematic uncertainties are considered.

- The model dependence of the acceptance is determined using the angular distributions, which are specific for each particular model. As shown in Sec. 4, a model with one $\rho(770)$ and remaining pions in S-wave (phase space or $f_0(1370)$) gives good overall agreement with the observed angular distributions. Using the ratio of six- and five-track events we estimate a systematic uncertainty on the detection efficiency as 4%.

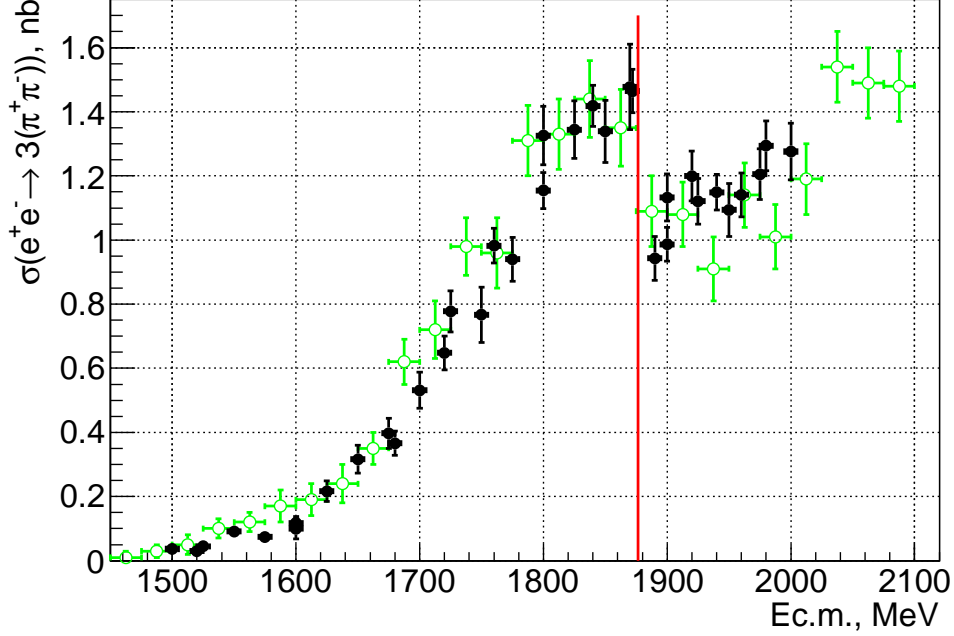


Figure 7: The $e^+e^- \rightarrow 3(\pi^+\pi^-)$ cross section measured with the CMD-3 detector at VEPP-2000 (dots). The results of the BaBar measurement [2] are shown by open circles. The line shows the $p\bar{p}$ threshold.

- Since only one charged track is sufficient for a trigger (99-98% efficiency), we assume that for the multi-track events, considered in this analysis, the trigger inefficiency gives a negligible contribution to the systematic error.
- A systematic error due to the selection criteria is studied by varying the cuts described previously and doesn't exceed 3%.
- The uncertainty on the determination of the integrated luminosity comes from the selection criteria of Bhabha events, radiative corrections and calibrations of DC and CsI and does not exceed 2% [14].
- The admixture of the background events not subtracted from the six-track sample is estimated as 1%.

- The accuracy of background subtraction for five-track events is studied by the variation of functions used for a background description in Fig. 1(d) and is estimated as 3%.
- A possible uncertainty on the beam energy is studied using the momentum distribution of Bhabha events and total energy of four-pion events. The uncertainty at the level of $5 \cdot 10^{-3}$ is not excluded and because of the cross section variation it can result in a 1% change of the cross section.
- A radiative correction uncertainty is estimated as about 1% mainly due to the uncertainty on the maximum allowed energy of the emitted photon, as well as from the uncertainty on the cross section.

The above systematic uncertainties summed in quadrature give an overall systematic error of about 6%.

The obtained cross section is in overall agreement with the results of the most precise measurement performed by the BaBar Collaboration [2] shown in Fig. 7 by open circles.

Conclusion

The total cross section of the process $e^+e^- \rightarrow 3(\pi^+\pi^-)$ has been measured using 22 pb^{-1} of integrated luminosity collected by the CMD-3 detector at the VEPP-2000 e^+e^- collider in the 1.5-2.0 GeV c.m. energy range. The five- and six-track events are used to estimate the model-dependent uncertainty in the acceptance calculation. From our study we can conclude that the observed production mechanism can be described by the production of one $\rho(770)$ with four remaining pions in S-wave and distributed according to phase space. We also observe that the production dynamics changes in the 1700-1900 MeV c.m.energy range and demands further investigation. A detailed analysis of the production dynamics will be performed in the combined analysis of the processes $e^+e^- \rightarrow 3(\pi^+\pi^-)$ and $e^+e^- \rightarrow 2(\pi^+\pi^-)2\pi^0$.

The measured cross section is in good agreement with all previous experiments in the energy range studied, and exhibits a sharp dip near the $p\bar{p}$ threshold.

Acknowledgements

The authors are grateful to A.I. Milstein and Z.K. Silagadze for their help with a theoretical interpretation and development of the models. We thank the VEPP-2000 team for excellent machine operation.

This work is supported in part by the Russian Education and Science Ministry, by FEDERAL TARGET PROGRAM "Scientific and scientific-pedagogical personnel of innovative Russia in 2009-2013", by agreement 14.B37.21.07777, by the Russian Fund for Basic Research grants RFBR 10-02-00695-a, RFBR 10-02-00253-a, RFBR 11-02-00328-a, RFBR 11-02-00112-a, RFBR 12-02-31501-a, RFBR 12-02-31499-a, RFBR 12-02-31498-a, and RFBR 12-02-01032-a.

REFERENCES

- [1] R. Baldini *et al.*, reported at the "Fenice" Workshop, Frascati (1988). A. B. Clegg and A. Donnachie, *Z. Phys. C***45**, 677 (1990). M.R. Whalley, *J. Phys. G***29**, A1 (2003).
- [2] B. Aubert *et al.* (BaBar Collaboration), *Phys. Rev. D***73**, 052003 (2006).
- [3] P.L. Frabetti *et al.* (FOCUS Collaboration), *Phys. Lett. B***514**, 240 (2001).
- [4] P.L. Frabetti *et al.* (FOCUS Collaboration), *Phys. Lett. B***578**, 290 (2004).
- [5] B. Aubert *et al.* (BaBar Collaboration), *Phys. Rev. D***73**, 012005 (2006).
- [6] A. Sibirtsev and J. Haidenbauer, *Phys. Rev. D***71**, 054010 (2005).
- [7] A. Antonelli *et al.* (FENICE Collaboration), *Phys. Lett. B***365**, 427 (1996).
- [8] M. Davier, S. Eidelman, A. Höcker, Z. Zhang, *Eur. Phys. J. C***31**, 503 (2003).

- [9] V.V. Danilov *et al.*, Proceedings EPAC96, Barcelona, p.1593, (1996).
I.A.Koop, Nucl. Phys. B (Proc. Suppl.), **181-182**, 371 (2008).
- [10] B.I.Khazin, Nucl. Phys. B (Proc. Suppl.), **181-182**, 376 (2008).
- [11] F. Grancagnolo *et al.*, Nucl. Instr. and Meth. A, **623**, 114 (2010).
- [12] A.V.Anisyonkov *et al.*, Nucl. Instr. and Meth. A, **598**, 266 (2009).
- [13] D. Epifanov (CMD-3 Collaboration), J. Phys. Conf. Ser. **293**, 012009, (2011).
- [14] R.R. Akhmetshin *et al.*, Nucl. Phys. B (Proc. Suppl.), **225-227**, 69 (2012).
- [15] S. Agostinelli *et al.* (GEANT4 Collaboration), Nucl. Instr. and Meth. A, **506**, 250 (2003).
- [16] R.R. Akhmetshin *et al.* Preprint BudkerINP 98-83, Novosibirsk 1998; Phys. Lett. B**466**, 392 (1999).
- [17] J. Beringer *et al.* (Particle Data Group), Phys. Rev. D**86**, 1 (2012).
- [18] E.A. Kuraev and V.S. Fadin, Sov. J. Nucl. Phys. **41**, 466 (1985).

Table 1: Luminosity, Number of events, Detection efficiency, Rad. correction and Cross section for each c.m. energy point. Horizontal lines separate three energy scans.

Ec.m. , MeV	L, nb⁻¹	N_{6π}	N_{5π}	ε_{MC}	1 + δ	σ, nb
2000	474.7	88	166.0±14.8	0.480	0.905	1.28±0.09
1975	516.5	95	168.4±14.3	0.484	0.906	1.20±0.08
1950	458.8	91	124.8±13.2	0.488	0.913	1.09±0.08
1925	582.2	110	179.4±15.0	0.492	0.934	1.12±0.07
1900	495.6	104	155.1±13.5	0.496	0.964	1.13±0.07
1850	431.8	94	156.9±15.3	0.504	0.892	1.34±0.10
1800	440.1	86	168.6±15.0	0.513	0.883	1.33±0.09
1750	541.8	54	126.2±18.9	0.513	0.877	0.77±0.09
1700	486.1	38	72.5±10.0	0.513	0.865	0.53±0.06
1650	463.3	21	42.3±7.5	0.513	0.873	0.32±0.04
1600	441.9	9	10.5±5.5	0.513	0.900	0.099±0.032
1550	521.1	9	12.1±4.0	0.505	0.914	0.091±0.013
1500	554.6	3	5.9±4.1	0.497	0.921	0.037±0.018
1890	521.5	95	137.4±13.7	0.498	0.984	0.94±0.07
1870	663.4	163	259.1±35.9	0.501	0.891	1.48±0.13
1825	500.8	113	179.1±16.5	0.509	0.885	1.34±0.09
1775	550.7	85	139.7±13.5	0.513	0.878	0.94±0.07
1725	523.0	70	104.6±11.7	0.513	0.867	0.78±0.06
1675	561.4	32	63.4±9.8	0.513	0.865	0.40±0.05
1625	508.5	16	32.4±6.1	0.513	0.888	0.22±0.03
1575	522.2	7	10.2±3.5	0.509	0.907	0.074±0.011
1525	530.9	3	7.5±3.3	0.501	0.920	0.045±0.016
1980	602.2	111	217.9±16.5	0.484	0.905	1.29±0.08
1960	680.1	117	214.6±16.7	0.487	0.910	1.14±0.07
1940	988.7	173	322.4±20.2	0.490	0.923	1.15±0.06
1920	491.5	90	171.8±14.0	0.493	0.934	1.20±0.08
1900	883.3	145	257.1±17.7	0.496	0.964	0.99±0.05
1872	845.6	193	340.0±20.2	0.501	0.891	1.46±0.07
1840	952.1	197	390.7±22.4	0.506	0.892	1.42±0.06
1800	972.1	157	332.6±20.6	0.513	0.883	1.15±0.06
1760	950.4	153	252.2±18.7	0.513	0.878	0.98±0.05
1720	797.4	95	126.5±15.3	0.513	0.867	0.65±0.05
1680	879.2	58	79.7±12.0	0.513	0.865	0.37±0.04
1600	812.7	10	32.4±6.5	0.513	0.900	0.117±0.020
1520	825.3	2	8.9±3.6	0.500	0.920	0.030±0.011